

## A NEW MODEL IN $\theta$ -STOCK TO SIMULATE THCM BEHAVIOR IN OIL TRANSFER WITHIN FUNICULAR ZONE

Touraj Tayebi\* and Behrouz Gatmiri\*,†

\* Center of Excellence for Engineering and Management of Infrastructures(CE-EMI)  
Department of Civil Engineering , University of Tehran, Enghelab Ave., Tehran, Iran  
e-mail: tayebie@gmail.com, web page: <http://www.ut.ac.ir>

† Université de Paris-Est, Institut Navier, Ecole Nationale des Ponts et Chaussées  
6-8 Ave. Blaise Pascal , 77455 Marne la Vallee cedex 2, Paris, France  
e-mail: [gatmiri@cermes.enpc.fr](mailto:gatmiri@cermes.enpc.fr), web page: <http://www.enpc.fr>

**Key words:** Theta-STOCK FE code, unsaturated soil mechanics, oil transfer, deformable porous media, THCM(Thermal/Hydraulic/Chemical/Mechanical) interactions

**Summary.** This article presents the model used in the development of  $\theta$ -STOCK program for application on the problem of oil flow through porous media and briefly acquaints readers with verification and application of the modified program on complex scenarios of light oil flow through funicular(continuous capillary) zone of unsaturated soils in subsurface aquifers.

### 1 INTRODUCTION

Mechanics of unsaturated soils is a fast growing area of research in soil mechanics which has its application in many allied fields of engineering such as geotechnical, water resources, environmental, and petroleum engineering<sup>1, 2, 3</sup>. These fields have one of their interfaces in the subject of contaminant flow through porous media. Taking a brief look at the prior attempts in this area shows a great deal of evolution in the phases which have been taken into account and the methods dealing with their consideration, yet little are those considering the effect of heat alteration and soil structure deformation on the subject of multi-phase flow in unsaturated underground aquifers. The THCM model introduced in the present paper is implemented in the  $\theta$ -STOCK program as a development of the prior THM model<sup>4, 5, 6, 7, 8</sup> whose governing equations are fully coupled with each other by the use of state surfaces concept. The formulation of state surfaces of void ratio (VRSS<sup>1</sup>) and degree of saturation (DSSS<sup>2</sup>) have been presented by Gatmiri<sup>4, 5</sup> for gas-water interface on the basis of experimental researches in CERMES. Based on water retention curves (WRCs) presented for NAPL-water interfaces<sup>9</sup>, the DSSS formulation has been modified and extended by Tayebi and Gatmiri<sup>1, 2, 3</sup> in the new THCM model. Another major issue to deal with in deformable porous media is the non-linearity of the elastic deformable soil which is considered here by the employment of Kondner-Duncan (hyperbolic) model<sup>4</sup>. For the sake of brevity of the text, the literature review is omitted from here and addressed to prior works of the authors<sup>3, 4, 5, 7, 8</sup>.

## 2 THE PROPOSED MODEL AND SOLUTION

Governing equations of our THCM model consist of first (equilibrium and flow equations) and second (constitutive and conservation equations) thermodynamic laws written for three phases of soil particles, water, oil (NAPL), and the term of heating. These equations are presented in Table 1 in which inadequacy of equations versus unknowns is obvious<sup>1,3</sup>. Indeed, this set of equations is not complete without the equations of state which are given in Table 2 as well as secondary equations<sup>3</sup>. These set of equations are solved by means of finite element method. Bubnov-Galerkin integral forms of field equations are used for spatial and temporal discretized matrix form of the equilibrium equations, and implicit integration scheme is used in time to consider their non-linearity. The algorithm of  $\theta$ -STOCK which is based on the current THCM model is shown in Figure 1 in which the shaded areas are modules which have been developed, modified, or added to the prior THM-based code to solve the new THCM model<sup>3,7</sup>. The suffix of AXI shows the modules used for axi-symmetric analysis which is not used for integration of the THCM model in the code of  $\theta$ -STOCK. The code is prepared for plain-strain analysis. More details for the STIFF subroutine which calculates the stiffness matrix is presented in the top-right part of Figure 1. The subroutines in which VRSS and DSSS are calculated are STATEVT and STATEST, respectively, whose formulation for our THCM model is presented in the last two rows of Table 2.

Main governing equations		Number of	
		Equations <sup>a</sup>	Unknowns <sup>b</sup>
Equilibrium of solid skeleton	$\left( \underline{\underline{\underline{\underline{\sigma}}}}_{ij} - \underline{\underline{\underline{\underline{\delta}}}}_{ij} \cdot \underline{\underline{\underline{\underline{P}}}}_n \right) + \underline{\underline{\underline{\underline{P}}}}_{ni} + \underline{\underline{\underline{\underline{b}}}}_i = 0$	3	5 <sup>c</sup>
Soil constitutive law	$d \left( \underline{\underline{\underline{\underline{\sigma}}}}_{ij} - \underline{\underline{\underline{\underline{\delta}}}}_{ij} \cdot \underline{\underline{\underline{\underline{P}}}}_n \right) = \underline{\underline{\underline{\underline{D}}}} \cdot d \underline{\underline{\underline{\underline{\epsilon}}}} - \underline{\underline{\underline{\underline{F}}}} \cdot d \left( \underline{\underline{\underline{\underline{P}}}}_n - \underline{\underline{\underline{\underline{P}}}}_w \right) - \underline{\underline{\underline{\underline{C}}}} \cdot d \underline{\underline{\underline{\underline{T}}}}$	3	8 <sup>d</sup>
Water conservation law	$\frac{\partial (\underline{\underline{\underline{\underline{\theta}}}} \cdot \underline{\underline{\underline{\underline{\rho}}}}_w)}{\partial t} = -\underline{\underline{\underline{\underline{\nabla}}}} \cdot (\underline{\underline{\underline{\underline{\rho}}}}_w \cdot \underline{\underline{\underline{\underline{U}}}})$	1	1
Water flow equation	$\underline{\underline{\underline{\underline{U}}}} = \frac{q_w}{\rho_w} = -\underline{\underline{\underline{\underline{D}}}}_{rw} \cdot \underline{\underline{\underline{\underline{\nabla}}}} T - \underline{\underline{\underline{\underline{D}}}}_{\theta w} \cdot \underline{\underline{\underline{\underline{\nabla}}}} \theta - \underline{\underline{\underline{\underline{D}}}}_w \cdot \underline{\underline{\underline{\underline{\nabla}}}} Z$	1	3
NAPL conservation law	$\frac{\partial}{\partial t} \left[ (\underline{\underline{\underline{\underline{n}}}} - \underline{\underline{\underline{\underline{\theta}}}}) \cdot \underline{\underline{\underline{\underline{\rho}}}}_n \right] = -\underline{\underline{\underline{\underline{\nabla}}}} \cdot (\underline{\underline{\underline{\underline{\rho}}}}_n \cdot \underline{\underline{\underline{\underline{V}}}})$	1	3
NAPL flow equation	$\underline{\underline{\underline{\underline{V}}}} = \frac{q_n}{\rho_n} = -\underline{\underline{\underline{\underline{D}}}}_{rn} \cdot \underline{\underline{\underline{\underline{\nabla}}}} T - \underline{\underline{\underline{\underline{D}}}}_{pn} \cdot \underline{\underline{\underline{\underline{\nabla}}}} P_n - \underline{\underline{\underline{\underline{D}}}}_n \cdot \underline{\underline{\underline{\underline{\nabla}}}} Z$	1	3
Energy conservation law	$\frac{\partial \underline{\underline{\underline{\underline{\Phi}}}}}{\partial t} + \text{div} \cdot (\underline{\underline{\underline{\underline{Q}}}}) = 0$	1	2
Heat flow	$\underline{\underline{\underline{\underline{Q}}}} = -\underline{\underline{\underline{\underline{\lambda}}}} \cdot \underline{\underline{\underline{\underline{\nabla}}}} T + [C_{pw} \cdot \underline{\underline{\underline{\underline{\rho}}}}_w \cdot \underline{\underline{\underline{\underline{U}}}} + C_{pn} \cdot \underline{\underline{\underline{\underline{\rho}}}}_n \cdot \underline{\underline{\underline{\underline{V}}}}] \cdot (T - T_0)$	1	1
Total number of equations and unknowns for the main governing equations:		12	26

<sup>a</sup> The number of underlines shows the dimension of each parameter (one for vectors; two for matrices).

<sup>b</sup> The number of caps above each parameter shows the number of associated unknowns to it.

<sup>c</sup> Unknowns of stress tensor are:  $\sigma_{11}$ ,  $\sigma_{13}$ ,  $\sigma_{33}$ , and  $\sigma_{22}$ .

<sup>d</sup> Unknowns of strain tensor, under plain strain situation, are:  $\epsilon_{11}$ ,  $\epsilon_{13}$ , and  $\epsilon_{33}$ .

Table 1: Summary of the equations and unknowns of the main governing equations

The new equations of state, whose compatibility with the code has been approved in prior works, are the key in coupling different phases' responses with each other. How this process

works is partly presented in Figure 2. As it is shown in Figure 2(c), hydraulic conductivity of the medium with regard to water and oil is a function of void spaces, temperature, and degree of saturation. On the other hand, the concept of state surfaces which is presented in Figures 2(a) and 2(b) will connect the mechanical, hydraulic, chemical, and thermal domains with each other as it is shown in Figures 2(d) and 2(e) in which hydraulic responses of water and the chemical phase are also a function of mechanical (stress-deformation) state of soil. A comprehensive discussion on this issue is presented in prior works<sup>1,2</sup>.

Complementary governing equations	Number of	
	Equations <sup>a</sup>	Unknowns <sup>b</sup>
-----Solid skeleton-----		
$\underline{\underline{D}} = \begin{pmatrix} \frac{3\bar{B}}{9\bar{B}-E} & \frac{3\bar{B}+E}{3\bar{B}-E} & 0 \\ \frac{3\bar{B}+E}{3\bar{B}-E} & \frac{3\bar{B}-E}{3\bar{B}+E} & 0 \\ 0 & 0 & E \end{pmatrix}$ ; $E = 3(1-2\nu) \cdot B$ ; $B = K_b \cdot P_{atm} \cdot \left(\frac{\sigma_3}{P_{atm}}\right)^m$ ; $\underline{\underline{m}}^T = [1 \ 1 \ 0]$	3	3
$\underline{\underline{C}} = \underline{\underline{D}} \cdot \underline{\underline{D}}_1^{-1}$ ; $\underline{\underline{D}}_1^{-1} = \underline{\underline{\beta}}_1 \cdot \underline{\underline{m}}$ ; $\beta_1 = \frac{1}{1+e} \cdot \frac{\partial e}{\partial T}$ ; $\underline{\underline{F}} = \underline{\underline{D}} \cdot \underline{\underline{D}}_s^{-1}$ ; $\underline{\underline{D}}_s^{-1} = \underline{\underline{\beta}}_s \cdot \underline{\underline{m}}$ ; $\beta_s = \frac{1}{1+e} \cdot \frac{\partial e}{\partial (P_n - P_w)}$	6	5
$E_L = (\bar{E}_i + \bar{E}_\psi + \bar{E}_T) \cdot (1 - R_f \cdot Sr)^2$ ; $E_i = K_L \cdot P_{atm} \cdot \left(\frac{\sigma_3}{P_{atm}}\right)^n$ ; $E_\psi = \beta \cdot (P_n - P_w)$ ; $E_T = m_1 \cdot T$	4	4
$\bar{E}_u = (\bar{E}'_i + E_\psi + E_T)$ ; $E'_i = K_u \cdot P_{atm} \cdot \left(\frac{\sigma_3}{P_{atm}}\right)^n$ ; $R_f = \frac{(\sigma_1 - \sigma_3)_f}{(\sigma_1 - \sigma_3)_{ult}}$ ; $Sr = \frac{\sigma_1 - \sigma_3}{(\sigma_1 - \sigma_3)_{ult}}$	4	3
$(\sigma_1 - \sigma_3)_f = \frac{2(\sigma_3 \cdot \sin \phi + c \cdot \cos \phi)}{1 - \sin \phi}$ ; $\bar{c} = c_{in} + m_2 \cdot (P_n - P_w)$ ; $\bar{\phi} = \bar{\phi}' \cdot \exp(0.002T)$	3	3
$\phi' = \begin{cases} \phi_{ult} & , \frac{P_n - P_w}{(P_n - P_w)_{ult}} \leq 1 \\ \phi_{ult} + (\phi_{in} - \phi_{ult}) \cdot \left[1 - \frac{P_n - P_w}{(P_n - P_w)_{ult}}\right]^2 & , \frac{P_n - P_w}{(P_n - P_w)_{ult}} > 1 \end{cases}$ ; $\sigma_x = \bar{K}_0 \cdot \sigma_y$	2	1
$K_0 = K_{nc} \cdot (OCR)^\rho$ ; $[(\bar{\sigma}_\alpha - P_n) - \frac{(\sigma_1 + \sigma_3 - P_n)}{2}]^2 + \tau_\alpha^2 = \left(\frac{\sigma_1 - \sigma_3}{2}\right)^2$ ; $\tau_\alpha = \left(\frac{\sigma_1 - \sigma_3}{2}\right) \cdot \sin(2\bar{\alpha})$	3	3 <sup>c</sup>
-----Water phase-----		
$D_{T_w} = \bar{K}_w \cdot \frac{\psi_{rf}}{\sigma_{rf}} \cdot \frac{d\sigma_{(T)}}{dT}$ ; $D_{\theta_w} = K_w \cdot \frac{\sigma_{(T)}}{\sigma_{rf}} \cdot \frac{d\psi_{rf}}{d\theta}$ ; $D_w = K_w$ ; $\psi_{rf} = \frac{P_w - P_n}{\gamma_w}$ ; $\sigma_{(T)} = -75.882 + 0.165T$	5	3
$K_w = a \cdot 10^{a \cdot e} \cdot \left[\frac{S_w - S_{w,r}}{1 - S_{w,r}}\right]^b \cdot \left(\frac{\mu_{w,rf}}{\mu_{w(T)}}\right)$ ; $\mu_{w(T)} = 0.6612(T - 229)^{-1.562}$ ; $\theta = n \cdot \bar{S}_w$ ; $n = \frac{e}{1+e}$	4	2
-----NAPL phase (Non-Aqueous Phase Liquid) -----		
$D_{T_n} = \frac{\bar{K}_n}{\gamma_n} \cdot \frac{\partial P_n}{\partial T}$ ; $D_{P_n} = \frac{K_n}{\gamma_n}$ ; $D_n = K_n$	3	1
$K_n = c \cdot \frac{\gamma_n}{\mu_{n,rf}} \cdot \left[e \cdot \left(\frac{1 - S_{n,r} - S_w}{1 - S_{n,r}}\right)\right]^d \cdot \left(\frac{\mu_{n,rf}}{\mu_{n(T)}}\right)$ ; $\mu_{n(T)} = \frac{\mu_{n,rf}}{\mu_{w,rf}} \times 0.6612(T - 229)^{-1.562}$ ; $n - \theta = n \cdot \bar{S}_n$	3	2
-----Heat term-----		
$\Phi = \bar{C}_T \cdot (T - T_0)$ ; $C_T = (1 - n) \cdot \rho_s \cdot C_{p_s} + \theta \cdot \rho_w \cdot C_{p_w} + (n - \theta) \cdot \rho_n \cdot C_{p_n}$	2	1
$\lambda = (1 - n) \cdot \lambda_s + \theta \cdot \lambda_w + (n - \theta) \cdot \lambda_n$	1	0
-----Couplement-----		
$e = (1 + e_0) \cdot \exp\left[-\frac{\left[a_c \cdot \left(\frac{\sigma - P_n}{P_{atm}}\right) + b_c \cdot \left(1 - \frac{\sigma - P_n}{\sigma_c}\right) \cdot \left(\frac{P_n - P_w}{P_{atm}}\right)\right]^{1-m}}{K_b \cdot (1 - m)}\right] \cdot \exp[-c_e \cdot (T - T_0)] - 1$	1	0
$S_w = (1 - S_{n,r} - S_{w,r}) \cdot \left\{1 - [1 + a_s \cdot (\sigma - P_n)] \cdot [1 - \exp(-b_s \cdot (P_n - P_w))] \cdot \exp[c_s \cdot (T - T_0)]\right\} + S_{w,r}$	1	0
<b>Total number of equations and unknowns for the complementary governing equations:</b>		<b>45</b> <b>31</b>
<b>Total number of equations and unknowns in the governing equations of the THCM model:</b>		<b>57</b> <b>57</b>

<sup>a</sup> The equations are separated by semicolons in each row.

<sup>b</sup> The number of caps above each parameter shows the number of associated unknowns to it.

<sup>c</sup>  $\sigma_\alpha = \sigma_{x\alpha}$ ,  $\sigma_y = \sigma_{y\alpha}$ ,  $\tau_\alpha = \tau_{xy}$ ,  $\tau_{yx}$ , and  $\alpha$  is the angle between horizontal or vertical plains with the principal stress plains.

Table 2: Summary of the equations and unknowns of the secondary governing equations

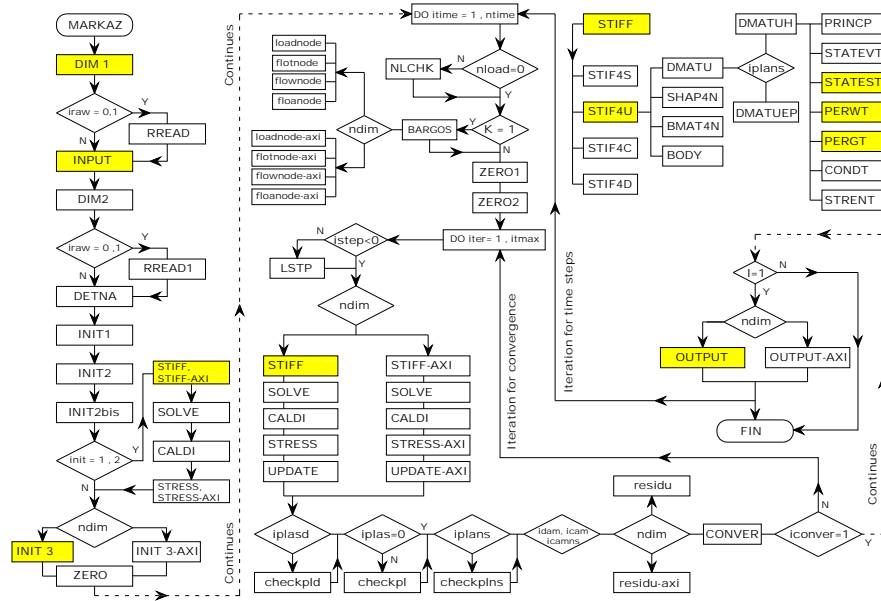


Figure 1: Global flowchart of  $\theta$ -STOCK FE Code and its stiffness matrix algorithm in plain strain module

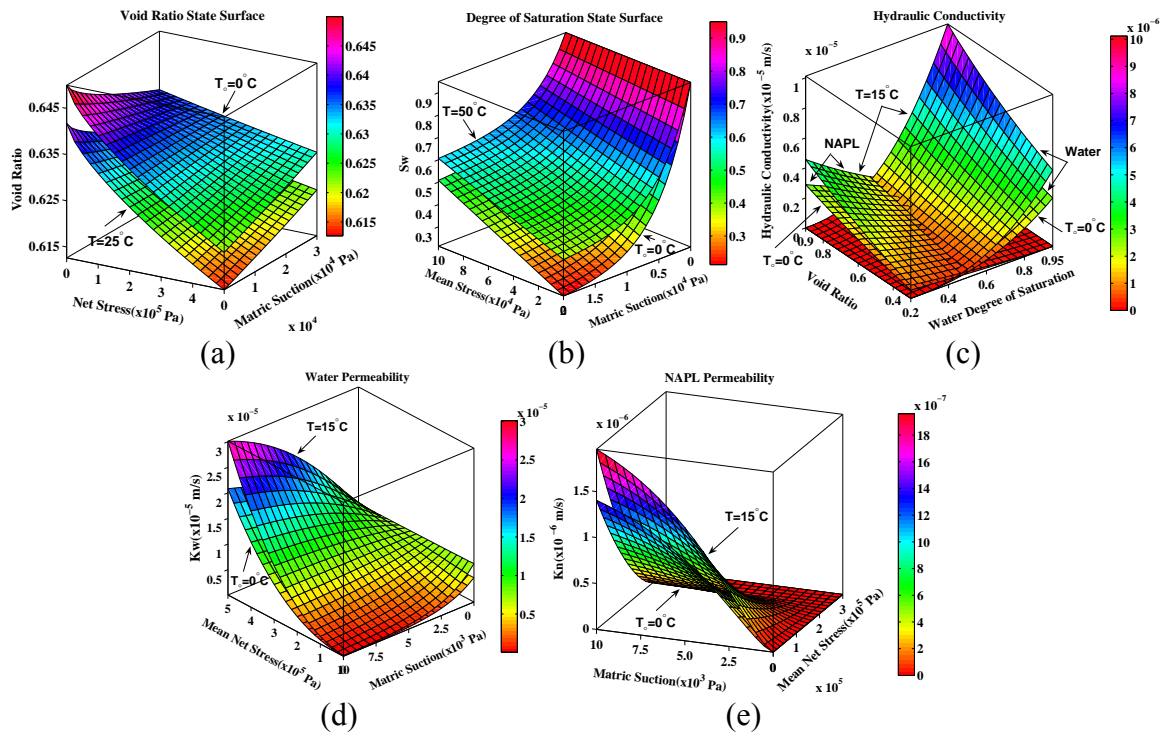


Figure 2: Fully coupled behavior of porous media via VRSS and DSSS concepts; (a) VRSS, (b) DSSS, (c) hydraulic conductivity (relative permeability) with regard to water and oil, (d) water permeability as a function of net stress as well as in (e) for oil permeability

### 3 JUSTIFICATION

Verification of the program in modeling the THM behavior of the medium, exposed in previous works of Gatmiri<sup>4,5,6,7,8</sup>, is widely accepted. To justify the results of the code for oil flow, a comparison between the solution of Lewis and Rahman<sup>9</sup> with the results of the present model is performed. Figure 3 shows the geometry, initial conditions, and boundary restrictions of the problem defined by Lewis and Rahman. The WRC (Water Retention Curve) and relative permeability functions for both models are presented in Figure 4. Finally, Figure 5 shows less than 10 percent difference between the results of the present THCM model and Lewis-Rahman's, which leads us to apply the THCM model on new problems.

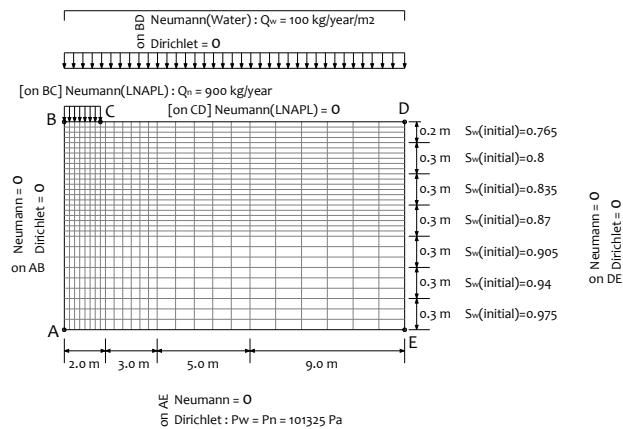


Figure 3: Geometry, initial conditions, and boundary restrictions of the verification problem

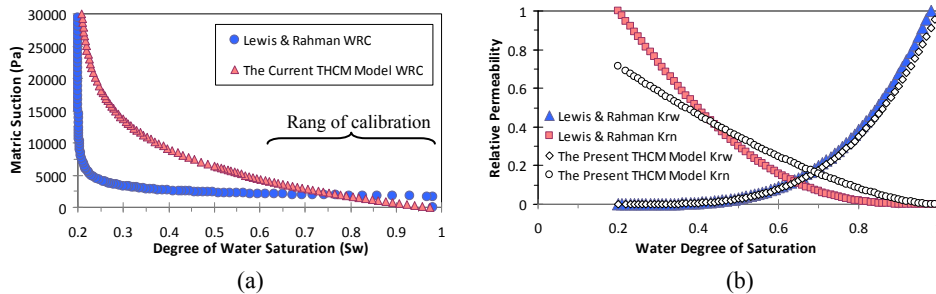


Figure 4: Calibration of input data; (a) DSSS and WRC, (b) relative permeability of oil and water

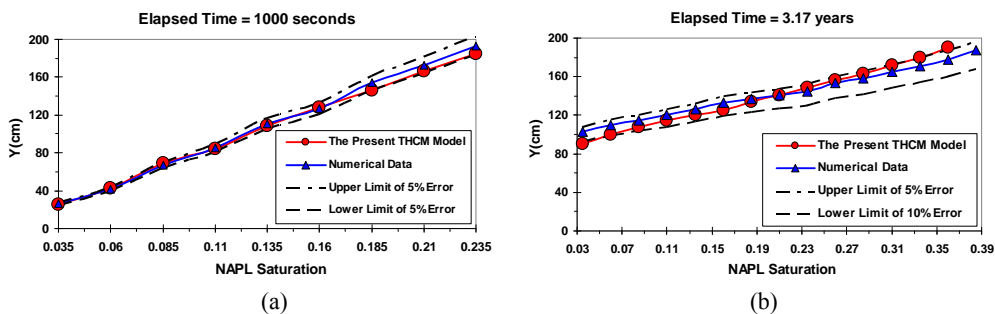


Figure 5: Comparison of NAPL concentration results of current model with Lewis-Rahman's ; after (a) 1000 seconds, (b) 3.17 years

#### 4 APPLICATION

The geometry of the medium along with its initial and boundary conditions are depicted in Figure 6. From the middle-top part of the medium (BC), kerosene, a thin oil product widely used in airplane jet engines, which is among LNAPLs (Lighter than water NAPLs) is under constant pressure to enter the medium, whereas beneath the leakage source a quite impermeable lens (GHIJ) is placed. The problem is solved for two scenarios of multi-phase flow: the first scenario is for isothermal condition (Case 1), and the second scenario will be for non-isothermal situation (Case 2) in which the medium is under heating from a core (KLMN) in the middle of the impermeable zone. More details could be followed in Figure 6.

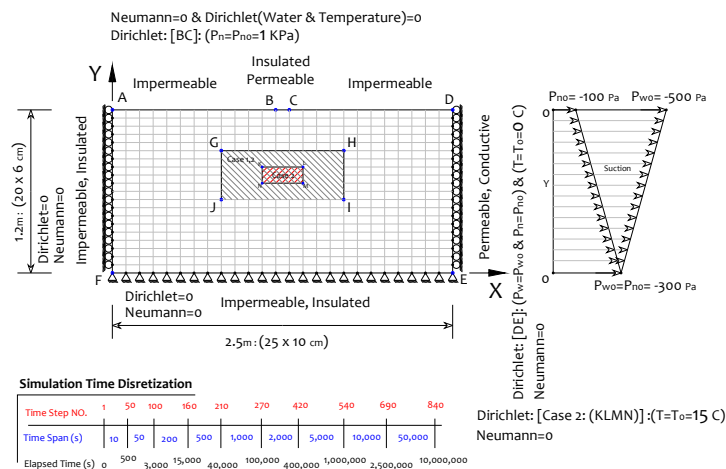


Figure 6: Geometry, initial conditions, and boundary restrictions in simulation of isothermal (Case 1) and non-isothermal (Case 2) oil-water flow through deformable soil

#### 4.1 Results and Discussions

Figure 7 presents the results for both scenarios as pollutant degree of saturation contours in different times. Figures 7(a) to 7(c) show the results for the first scenario, and Figures 7(d) to 7(f) present the results for the second scenario. As temperature increase approaches the contaminant dissipation front, a recess occurs in NAPL flow which is apparent in Figure 7(e). As time passes, the difference between two scenarios increases until the medium and leakage source are disconnected from each other, shown in Figure 7(f) in which the remaining NAPL is pulled to the left side of the medium.

Figure 8 depicts the temperature isopleths at the end of simulation. To show how complex the interactions in THCM behavior modeling are, Figures 9(a) and 9(b) are presented. Figure 9(a) shows the changes of water and oil conductivity through time for each case, all together. The compatibility in rises and falls of each phase's conductivity puts on view one of the main concepts of our THCM model which directly will affect dispersion of each phase's concentration through the porous medium., Figure 9(b) displays the changes of NAPL saturation over time for both cases along with the changes of temperature.

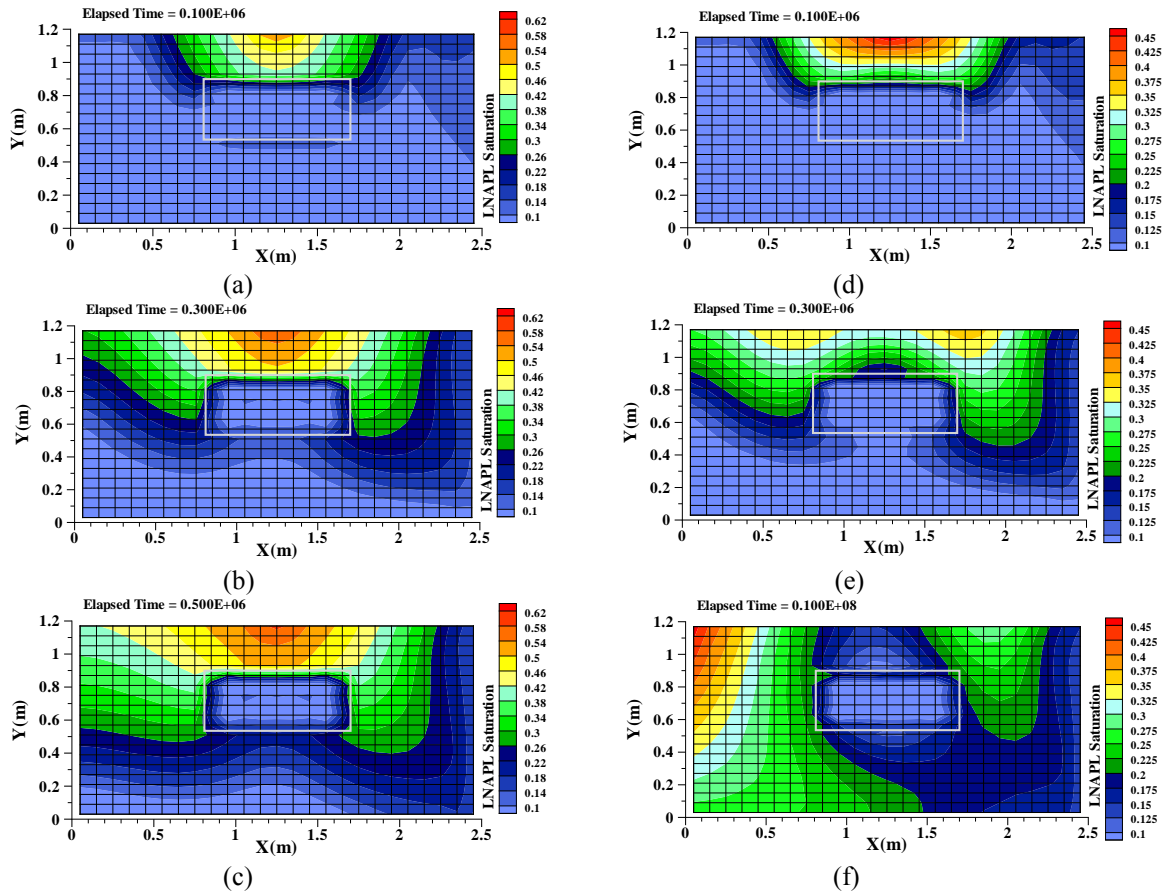


Figure 7: Oil concentration contours at different times for (a,b,c) isothermal (Case 1), and (d,e,f) non-isothermal conditions (Case 2)

Figure 9(b) shows the involvement of stress and temperature states in the hydraulic response of the medium by influencing the permeability of the medium with regard to both water and NAPL. Once heat loading approaches the oil dissipation front, the rate of contamination decreases until the connection between oil leakage source and the medium is jammed with dominance of water in such zones. Both sensitivity of heat flow to hydraulic response of the media and insensitivity of heat flow to mechanical domains are exposed in prior applications of the program<sup>1, 2, 3</sup>.

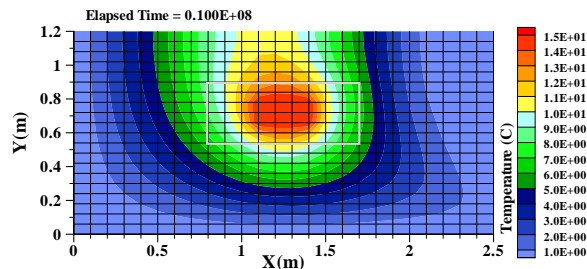


Figure 8: Heat distribution in the medium at the end of simulation time

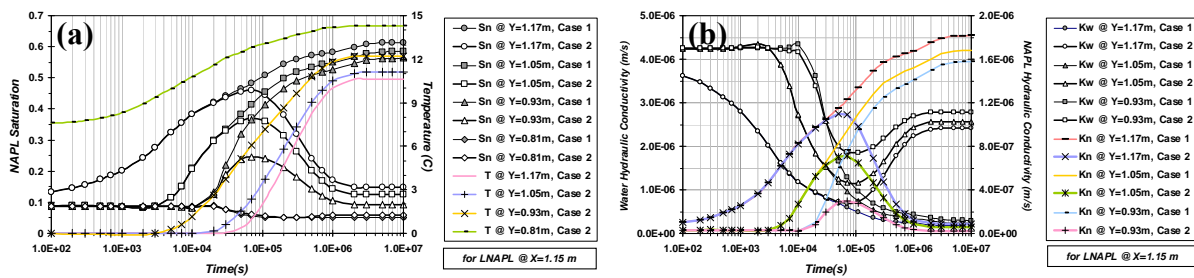


Figure 9: Results of  $\theta$ -STOCK application for (a) hydraulic conductivity, and (b) oil concentration versus time

## 5 CONCLUSIONS

- The algorithm of  $\theta$ -STOCK and its developed THM model to new fully coupled THCM model are presented in detail along with the concept of state surfaces.
- Comparison between the present THCM model and other verified models show great agreement between the results.
- Application of the proposed THCM model on new scenarios of thermal oil flow through deformable porous media approves the unique capability of the current model in simulation of NAPL transfer within funicular zone of oil contaminated aquifers.

## REFERENCES

- [1] T. Tayebi and B. Gatmiri, *Thermal void ratio state surface effect on immiscible fluid (NAPL) flow through unsaturated poroelastic media*, 8th International Congress on Civil Engineering, May 11-13, 2009, Shiraz University, Shiraz, Iran, (2009).
- [2] T. Tayebi and B. Gatmiri, *Water retention curve effect on the deformable porous media response to migration of NAPL under non-isothermal immiscible multi-phase flow situation*, 4th Biot Conference on Poromechanics, June 8-10, Columbia University, NY, USA, (2009).
- [3] T. Tayebi, *Numerical modeling of hydrocarbure contaminant transport through unsaturated multi-phasic porous media*, M.Sc. thesis, University of Tehran, Iran, (2009).
- [4] B. Gatmiri, *Analysis of fully coupled behavior of unsaturated porous media under stress, suction, and temperature gradient*, Final Report, CERMES, ENPC, Paris, (1997).
- [5] B. Gatmiri and P. Delage, *A formulation of fully coupled thermal-hydraulic-mechanical behavior of saturated porous media-numerical approach*, Int. J. Numer. Anal. Meth. Geomech., **21**(3), 199-225, (1997).
- [6] B. Gatmiri and A. Hoor, *Effect of excavation on the thermohydromechanical behaviour of a geological barrier*, Physics and Chemistry of the Earth J., **32**, 947-956, (2007).
- [7] B. Gatmiri and C. Arson,  *$\theta$ -STOCK, a powerful tool of thermohydromechanical behaviour and damage modelling of unsaturated porous media*, Computers and Geotechnics, **35**, 890-915, (2008).
- [8] B. Gatmiri and M. Najari, *Modeling of settlement and induced matric suction in multiphase porous media under root water uptake effect by F.E.M*, Commun. Numer. Meth. Engng, Published online in Wiley InterScience, DOI: 10.1002/cnm.1264, (2009).
- [9] N.A. Rahman and R.W. Lewis, *Finite element modelling of multiphase immiscible flow in deforming porous media for subsurface systems*, Computers and Geotechnics, **24**, 41-63, (1998).